GIS Odyssey Journal

2026 • Volume 6 • Number 1

https://doi.org/10.57599/gisoj.2026.6.1.193

Theresa Foley[1], Ann Marie Wolf[2], Palmira Henriquez[3], Imelda Cortez[4], Jella Balgos[5], Rachel Spitz[6]. Kevin Schaefer[7]

COMPARISON OF COMMUNITY SCIENCE RAIN GAUGE MEASUREMENTS WITH SATELLITE PRECIPITATION DATA IN TUCSON, ARIZONA, USA

Abstract: The Sonora Environmental Research Institute, Inc. (SERI) is a non-profit organization in Tucson, Arizona, USA. With the help of community scientists, SERI installed 168 rain gauges for a precipitation study in central Tucson. One hundred twelve or 67% of the participants met the U.S. Department of Housing and Urban Development (HUD) criteria for being low income. Forty-three percent of the participants spoke Spanish as their primary language, and 60% of participants identified as Hispanic. We compared the rain gauge data to NASA's Global Precipitation Measurement Mission (GPM) Integrated Multi-satellitE Retrievals for Global Precipitation (IMERG). The overall chi-square is 7.0 mm, indicating there is significant disagreement between the GPM and rain gauge measurements. We calculated an overall bias of 6 mm and an RMSE of 13 mm. We found that Tucson precipitation is variable in intensity and through space and time. A significant portion of this variability is below the resolution of the 9x11 kilometer GPM IMERG pixel.

Keywords: Precipitation, Global Precipitation Measurement (GPM), Integrated Multi-satellitE Retrievals for Global Precipitation (IMERG), Geographic information system (GIS), Community science

Received: 23 February 2026; accepted: 12 May 2026; revised: 7 June 2026

[1] Sonora Environmental Research Institute, Inc. (SERI), Tucson, Arizona, United States of America. ORCID ID: http://orcid.org/0000-0002-6796-3288, email: theresa.foley@seriaz.org, corresponding author
[2] SERI, Tucson, Arizona, USA, ORCID ID: http://orcid.org/0000-0002-1161-9146, email: Annmarie@seriaz.org
[3] SERI, Tucson, Arizona, USA, email: Palmira.henriquez@seriaz.org
[4] SERI, Tucson, Arizona, USA, email: imeldac@seriaz.org
[5] SERI, Tucson, Arizona, USA, email: jella@seriaz.org
[6] SERI, Tucson, Arizona, USA, email: rspitz@arizona.edu
[7] National Snow and Ice Data Center, Cooperative Institute for Research in Environmental Sciences (CIRES), University of Colorado, Boulder, Colorado, USA. ORCID ID: http://orcid.org/0000-0002-5444-9917, email: kevin.schaefer@colorado.edu

Introduction

The anthropogenic combustion of greenhouse gases has caused the average annual temperature of the American southwest to increase an average of 0.9°C between 1901 and 2016 (Gonzalez et al., 2018). The Sonoran Desert is experiencing increased minimum temperatures in the winter; a lengthening of the frost-free season; and a decreased frequency of freezing temperatures (Weiss & Overpeck, 2005). Higher temperatures are decreasing the soil moisture and increasing the aridity of this already arid region (Seager et al., 2007; Ault et al., 2016).

Rising temperatures are exacerbating the effects of the severe drought that the American southwest has been experiencing since 2000 (Overpeck & Udall, 2020). The 2000-2025 flow in the Colorado River, which supplies drinking water to seven states including Arizona, has decreased 19% below the 1906-2000 average (Silvertooth, 2025). Udall and Overpeck (2017) attribute approximately one-third of this decrease to human-caused climate change.

The city of Tucson obtains approximately 60% of its drinking water from the Central Arizona Project (CAP), which delivers Colorado River water to Tucson (City of Tucson, 2024). For Tucson, Arizona and other arid cities facing potential water scarcity, understanding the spatial and temporal variability of precipitation is crucial for managing and conserving precious water resources (Baghanam & Mohebbi, 2025). This project studies precipitation in metropolitan Tucson, using rain gauge data collected by community scientists. The rain gauge data is compared to NASA satellite images, National Weather Service (NWS) weather stations, and rain gauges from the Pima County Regional Flood Control District. The June 2023-October 2024 rain gauge data is also analyzed for correlation to latitude, longitude, elevation and percent tree canopy.

Materials and methods

Study area. Tucson, Arizona (32°13′18″N, 110°55′35″W) is an arid city, located 750 m above sea level within the Sonoran Desert, and 112 kilometers north of the United States-Mexico border. The city is located in a broad flat basin surrounded by four mountain ranges with elevations of up to 2500 meters, and it covers an area of 623 square kilometers (Comrie, 2000). The study area (Fig. 1) is directly west of the Davis Monthan Air Force Base and has an area of 791 kilometers. It includes the western side of Tucson, the one square mile city of South Tucson, and unincorporated Pima County. The Tohono Chul and Tucson International Airport weather stations are within the study area, and two additional Tucson weather stations are located outside the study area (Table 1).

The 1991-2020 annual precipitation average for Tucson is 269 mm (NWS, 2025). The Sonoran Desert is the only North American desert with two reliable rainy seasons. In winter it lies at the southernmost extreme of the polar-front jet stream, which moves midlatitude cyclonic storms through the area. During the summer, moisture from the North American Monsoon brings convective precipitation (Adams and Comrie, 1997 The hottest and driest time of year is from May to the beginning of the monsoon in late June or early July (Weiss et al., 2009).

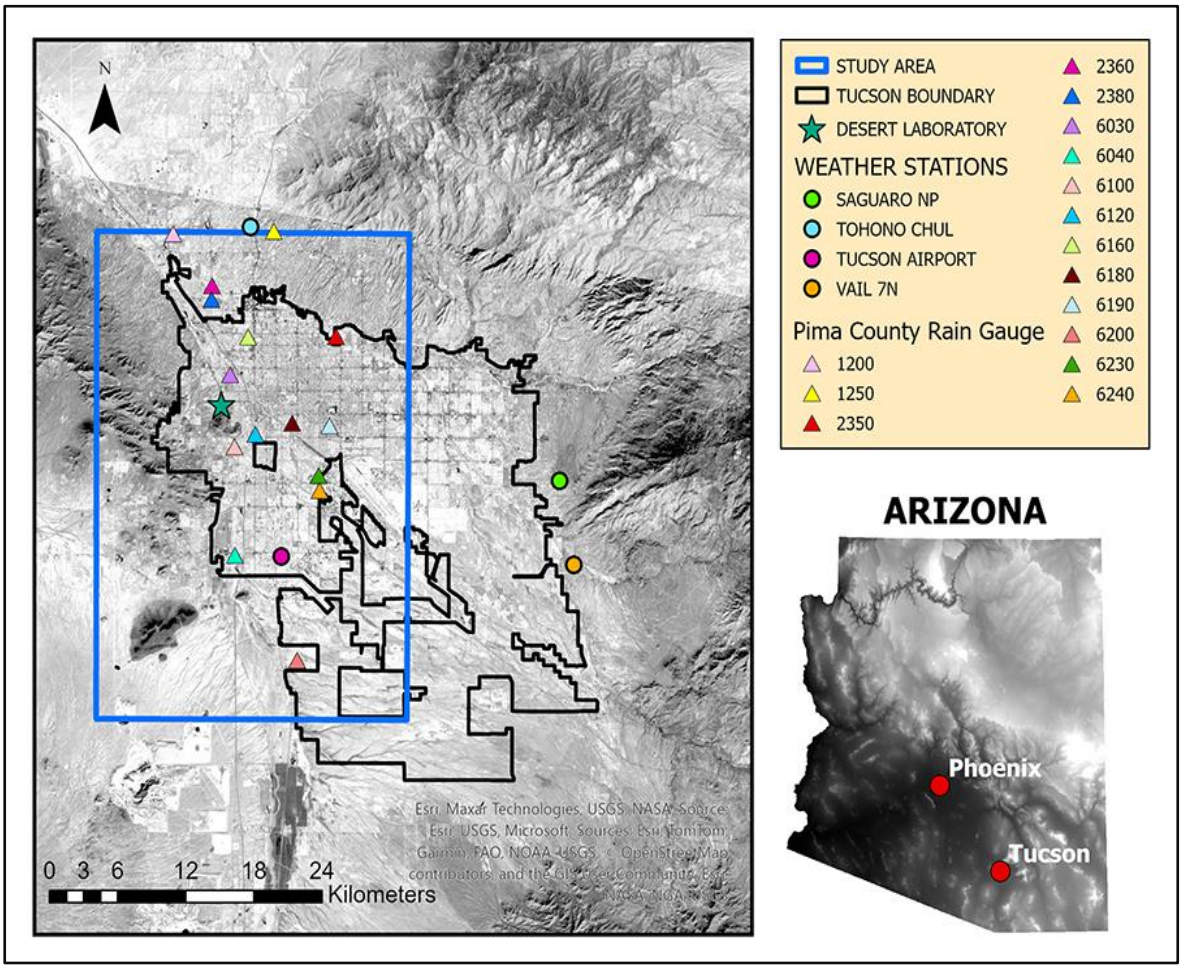

Fig. 1. Map of Study Area
Source: own elaboration based on Esri ArcGIS Online (2024), Arizona State University (n.d.)

Winter precipitation tends to be widespread, while summer monsoon precipitation is more variable and localized (Comrie & Broyles, 2002). Orographic effects (Baghanam & Mohebbi, 2025) and complex mountain-valley atmospheric circulation patterns (Comrie 2008) increase the variability of the monsoon precipitation. Climate change will probably cause Tucson to experience a decrease in average precipitation, while also experiencing more extreme precipitation events (Ghasemi Tousi et al., 2021).

Community science precipitation monitoring protocol. The Sonora Environmental Research Institute, Inc. (SERI) is a bilingual, non-profit community organization in Tucson, Arizona. Our mission is to develop a sustainable future by preserving the environment and protecting human health. We partner with the University of Arizona (Villagómez-Márquez et al., 2023) and other organizations to mitigate risks posed by environmental contamination and climate change. Our programs include tree planting in neighborhoods with limited green space (Foley et al., 2019) and low-income rainwater harvesting.

Community science is the process in which community members are involved in science as researchers (Conrad & Hilchey, 2011). We conducted a bilingual outreach to

recruit low income and Spanish speaking participants who are not easily reached by traditional outreach campaigns. Personal connections forged by our 30 years of work in southern metropolitan Tucson greatly assisted in recruiting participants.

Table 1. Tucson area locations measuring precipitation

Name	**ID**	**Latitude**	**Longitude**
Tucson Int. Airport (NWS)	USW00023160	32.1315	-110.9564
Tohono Chul (NWS)	USC00028590	32.3391	-110.9808
Saguaro National Park (NWS)	USC00027398	32.1794	-110.7363
Vail 7N (NWS)	USC00028998	32.1263	-110.7247
Canada Del Oro at Ina Road (PCRFD)	1200	32.3355	-111.0420
Pima Wash at Ina Road (PCRFD)	1250	32.3371	-110.9624
Rillito Creek above Dodge Blvd (PCRFD)	2350	32.2709	-110.9131
Rillito Creek at La Cholla Blvd (PCRFD)	2360	32.3029	-111.0112
Ruthraff Road near La Cholla Blvd (PCRFD)	2380	32.2941	-111.0117
Santa Cruz River above Grant Road (PCRFD)	6030	32.2468	-110.9969
Santa Cruz River at Valencia Road (PCRFD)	6040	32.1331	-110.9931
Mission Road near Silverlake Road - Santa Cruz Basin (PCRFD)	6100	32.2015	-110.9934
W. 20th St near I-10 (PCRFD)	6120	32.2093	-110.9769
Tom Meixner Memorial at Holy Hope Cemetery (PCRFD)	6160	32.2705	-110.9827
Arroyo Chico Wash at Cherry Avenue (PCRFD)	6180	32.2163	-110.9478
Arroyo Chico Wash at Randolph Park (PCRFD)	6190	32.2147	-110.9183
Summit Elementary - Franco Basin (PCRFD)	6200	32.0669	-110.9439
Tucson Diversion Channel at Ajo Detention Basin (PCRFD)	6230	32.1833	-110.9269
Kino Medical – Tucson Diversion Basin (PCRFD))	6240	32.1739	-110.9261

Source: own elaboration based on Northeast Regional Climate Center (2026), and Pima County Regional Flood Control District (2026)

Participants were provided with a 14 inch Stratus Precision Rain Gauge with Mounting Bracket, at a cost of $32.50 each. This model is recommended by the US National Weather Service and the World Meteorological Organization (Drozdzioł & Absalon, 2023). The conventional mounting method is a wooden post about 60 cm above the ground (Drozdzioł & Absalon, 2023). In Tucson, the hard caliche soil makes digging post holes challenging. Instead, we created wooden mounts that fit securely over chain link, metal, and cinder block fences (Fig. 2). Rain gauges were installed in the open, away from trees and overhanging roofs. Our low-cost method provides more granular data in the target area where cost would be a barrier, giving more data points to evaluate the research questions.

Fig. 2. Rain Gauges with Fence Mount
Source: own elaboration

From May 2023 to October 2024, participants recorded precipitation every day it rained, and checked their rain gauge weekly during periods of no rain. We provided participants a variety of options for submitting their precipitation data because many participants lacked the Internet or a computer. We accepted rain gauge logs via email, text, WhatsApp, or SERI pickup. Participants received a grocery store gift card of $50 six months after receiving their rain gauge, and a $65 grocery store gift card at the end of the project. Participants who continued with the study after a year received a third $50 gift card.

Datasets used in this study. The Integrated Multi-satellitE Retrievals for Global Precipitation (IMERG) is a NASA algorithm that estimates global precipitation from the Global Precipitation Measurement (GPM) satellite constellation. GPM IMERG provides global coverage every half hour with a resolution of 0.1° (approximately 11.1 km north-south and 9.4 km east-west in Tucson). Early GPM IMERG data is available in 4-5 hours, and Late GPM IMERG data is available in 14-15 hours. The Final GPM IMERG data becomes available in 3 months in a geotiff format suitable for a geographic information system (GIS; Kelley, 2020). We downloaded May 2023 to November 2024 data from the NASA GPM web site (NASA, 2025).

In urban areas, hard imperious surfaces such as rooftops and asphalt increase the sensible heat flux. The increased atmospheric instability from the sensible heat flux may be offset by decreased evapotranspiration, possibly causing a decrease in precipitation (Yang et al., 2016). Urban trees can increase evapotranspiration and cool the built environment, but in arid cities such as Tucson the urban forest requires precious water resources for irrigation (Wei et al., 2026). To analyze the relationship between precipitation and the Tucson tree canopy, we used the Regional Tree Canopy database, which has a 1-meter resolution (Pima Association of Governments, 2008).

Pima County operates a system of automated rain gauges to support early-warning flood control. Hydrologists and emergency managers use this information for issuing timely warnings, closing roads, and keeping residents safe during monsoon season. The

county provided 2023 and 2024 precipitation data for comparison to our data (Pima County Regional Flood Control District, 2026).

Workflow and ArcGIS Pro 3.4.0 tools used. Rain gauge results were compiled in Excel, and imported into GIS using the *Excel to Table* and *XY Table to Point tools*. We used the World Geodetic System 1984 (WGS 1984) datum. This global model of the earth is used by most satellite and global positioning systems (Kumar, 1988).

Esri ArcGIS Pro can compute the value of a raster or polygon feature at individual points such as rain gauge locations. The *Extract Values to Points Tool* computed the corresponding precipitation measurement from the GPM IMERG satellite image. The Percent Tree Canopy is a polygon layer, and the *Spatial Join Tool* computed the tree canopy value at each rain gauge location.

Interpolation tools use point measurements such as precipitation to estimate values where there are no measurements. Interpolation is based upon Tobler's First Law of Geography. "Everything is related to everything else, but near things are more related than distant things" (Ahrens, 2006). When the spatial variation of a parameter is unknown, stochastic interpolation methods such as kriging are preferable to deterministic methods such as inverse distance weighing (Earls & Dixon, 2007; Meng et al., 2013). Kriging is the generic name for a family of generalized least-squares regression algorithms, which create a mathematical function called a semi-variogram to describe how the data varies spatially (Li & Heap, 2011).

The *Ordinary Kriging Tool* has been widely used for interpolating rain gauge data because of its computational simplicity (Cheng et al., 2008; Haggag et al., 2016), but it assumes that the variation within the data does not vary spatially (Bostan, 2017). Gupta et al. (2017) instead recommend using the *Empirical Bayesian Kriging Tool* to interpolate precipitation data from arid areas because it is accurate for datasets with moderate spatial trends (Esri 2025).

Comparison with NASA GPM IMERG. We calculated the bias, root mean square error (RMSE), and chi-squared statistics. Bias represents the average difference between GPM IMERG and rain gauge data. RMSE represents the spread in variability between the GPM IMERG and measured precipitation. A lower bias and RMSE both indicate better performance. Chi-square is a goodness of fit test that evaluates whether differences between the GPM and rain gauge measurements are significantly different (Milton, 1999).

The residuals between GPM IMERG and each rain gauge measurement within each pixel are calculated as follows (Racka et al., 2013; Schaefer et al., 2015):

$$R_n = (P_{RS} - G_n) \tag{1}$$

Where:
R_n: residual for the n^{th} rain gauge measurement; P_{RS} is the GPM IMERG value; and G_n is the n^{th} rain gauge measurement in the pixel.

The chi-square for each pixel is:

$$\chi^2 = \frac{1}{N}\sum_{n=1}^{N}\frac{R_n^2}{\varepsilon^2} \tag{2}$$

Where:
X^2 is the chi-squared statistic for the pixel; N is the number of rain gauge measurements in the pixel; and ε is the uncertainty in the rain gauge measurements;
P_{RS} represents an average precipitation over a pixel while Gn represents point measurements of precipitation within the pixel. The representative error ε is the error that occurs when comparing point measurements such as rain gauge data to a satellite area average. We approximate ε as the standard deviation σ of G_n.

The ideal target for any remotely sensed data is to match *in situ* observations within the uncertainty. A chi-squared value less than one indicates that the satellite and rain gauge measurements are statistically identical (Racka et al., 2013; Schaefer et al., 2015). Variation within this target range has no physical meaning since the two measurements are statistically identical. A chi-squared value between one and four is a marginal match, indicating that the uncertainty bars overlap. A chi-squared value greater than four indicates that the two measurements do not match (Raczka et al., 2013). We calculated chi-square for every month of the 18-month the precipitation study. The monthly chi-squared value is the average chi-square of all the pixels within the study area.

Defining storm events and seasonal precipitation. ”Bursts” of monsoon precipitation tend to occur over a period of several days followed by a ”break” ranging from several days to several weeks (Mazon et al., 2016). We defined a winter or monsoon storm event as a period of two days or more in which 30% of the rain gauge measurements had a value of at least 0.05 inch (~1 mm). We analyzed the total precipitation of all the days in an event because participants checked their rain gauges at different times of the day. We defined the winter and monsoon seasons as follows (Baghanam & Mohebbi, 2025). The monsoon months are June through September, and winter months are October through March. Data from 1-2 April 2024 are included with the winter season data because the storm event began on 31 March 2024.

Linear regression models. To model the monsoon and winter precipitation datasets, we created generalized linear models (GLM). Our explanatory variables were latitude, longitude, and elevation (Comrie & Broyles 2002) as well as the percent tree canopy cover from the Regional Tree Canopy database. We used a gamma distribution with a log link function because precipitation in arid climates often has a gamma distribution rather than a normal distribution (Castro et al., 2009).

Modeling individual storm events required a different approach because the datasets contained many zero values when participants observed no precipitation. We performed a linear robust multivariate regression on each storm event, using the Matlab function Fitlm with the RobustOpts option on. Instead of minimizing the sum of squared residuals (which can be heavily skewed by outliers), robust regression assigns weights to each observation, giving less influence to values that deviate significantly from the model. Robust regression can also accommodate non-normal datasets (Yu & Yao, 2017).

Here is the general equation for both types of regression models:

$$Total_{mm} = 1 + \beta_0 + \beta_1 \cdot Lat + \beta_2 \cdot Lon + \beta_3 \cdot Z + \beta_4 \cdot Canopy + \sigma \qquad (3)$$

Where:
$Total_{mm}$ is the rain gauge measurement; Lat and Lon are the geographic coordinates; Z is the elevation; and Canopy is the percent tree canopy; B_0, β_1, β_2, β_3, and β_4 are the regression coefficients, and σ is the uncertainty.

Results and discussion

Results. The precipitation monitoring project began in May, 2023 and ended in October, 2024. We installed a total of 168 rain gauges, and 143 participants submitted at least some data logs, for an overall participation rate of 85% (Table 2). Sixty seven participants submitted data logs every month of the 18 month study, a very good participation rate for an extended study. The average total precipitation during the 17 month study is 418 mm, computed with data from the 67 participants (Table 3).

Table 2. Rain gauge data (mm) from all participants

Month	n	Avg.	Stdev.	Min.	Max.	Range	SE
May 2023	35	0.3	0.3	0.0	1.1	1.1	0.06
June 2023	111	0.7	7.0	0.0	73.4	73.4	0.66
July 2023	121	35.6	21.3	0.0	162.1	162.1	1.94
August 2023	125	37.9	19.3	0.0	85.7	85.7	1.73
September 2023	117	6.3	4.6	0.0	26.5	26.5	0.42
October 2023	113	9.4	11.0	0.0	55.4	55.4	1.04
November 2023	113	10.7	7.8	0.0	45.7	45.7	0.74
December 2023	111	36.6	11.8	2.5	99.3	96.8	1.12
January 2024	106	45.7	17.9	0.0	101.6	101.6	1.74
February 2024	100	38.3	10.8	6.9	77.7	70.9	1.08
March 2024	94	29.7	17.8	0.0	146.3	146.3	1.84
April 2024	91	16.0	8.2	0.0	35.1	35.1	0.86
May 2024	92	0.6	3.4	0.0	25.4	25.4	0.36
June 2024	87	45.4	45.4	0.0	422.9	422.9	4.87
July 2024	85	72.1	27.4	0.0	132.6	132.6	2.97
August 2024	84	33.6	17.8	0.0	103.9	103.9	1.94
September 2024	86	5.4	8.5	0.0	69.6	69.6	0.92
October 2024	84	0.1	0.6	0.0	5.8	5.8	0.07

Source: own elaboration

We compared our average monthly values to the four Tucson weather stations and the monthly average value of the 15 Pima County Regional Flood Control network in the study area (Table 1; Fig. 3). Because some of the datasets are not normally distributed, we used the non-parametric Kruskal Wallis test (Milton, 1999). The Tucson International Airport and the community data results are higher, but the difference is not statistically significant ($p=0.231$).

Table 3. Rain gauge data (mm) from the 67 participants with complete data

Month	Avg.	St. Dev.	Min.	Max.	Range	SE
June 2023	1	9	0	73	73	1.1
July 2023	34	14	0	79	79	1.7
August 2023	39	19	0	80	80	2.3
September 2023	7	5	0	27	27	0.6
October 2023	9	11	0	54	54	1.4
November 2023	10	5	0	33	33	0.6
December 2023	37	13	3	99	97	1.6
January 2024	47	16	0	102	102	2.0
February 2024	40	11	8	78	69	1.3
March 2024	28	13	0	82	82	1.5
April 2024	16	8	0	35	35	1.0
May 2024	0	2	0	18	18	0.3
June 2024	40	20	0	103	103	2.4
July 2024	73	25	0	133	133	3.1
August 2024	33	18	2	104	102	2.2
September 2024	6	9	0	70	70	1.1
October 2024	0	0	0	0	0	0.0
Total	418	66	191	635	444	8.1

Source: own elaboration

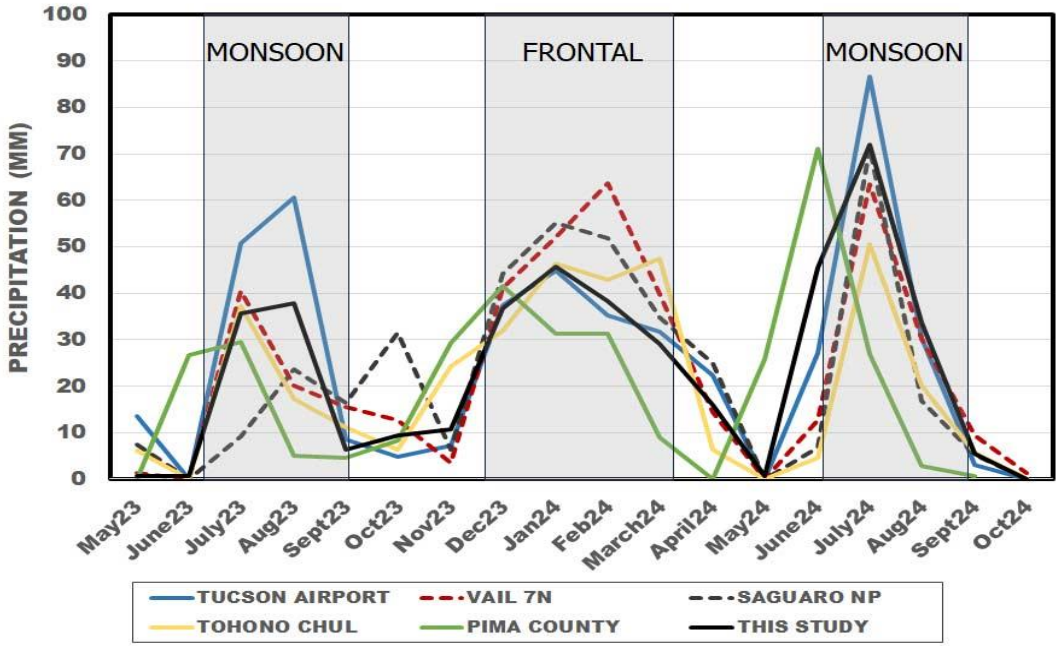

Fig. 3. Rain gauge data comparison
Sources: own elaboration based on Northeast Regional Climate Center (2026), and the Pima County Regional Flood Control District (2026)

We also compared our data to 1930–1933 rain gauge measurements of Humphrey (1933) at the Desert Laboratory on Tumamoc Hill, which is within the study area (see Fig. 1).

Humphrey placed 16 rain gauges at the base of Tumamoc Hill at approximately the same elevation as the rain gauges in this study, and eight additional gauges were placed in a straight line upslope about 200 meters. Figure 4 compares this study with the Humphrey data and the 1991-2020 average Tucson precipitation (National Weather Service, 2025). All of the datasets have the bimodal precipitation distribution characteristic of the Sonoran Desert (Adams & Comrie, 1997).

Our data and the Humphrey data have higher winter precipitation than the climatic norms. We attribute this to the strong June 2023-April 2024 El Niño event (Peng et al., 2025). El Niño is a climate pattern characterized by the unusual warming of surface waters in the central and eastern tropical Pacific Ocean. It is the warm phase of a larger climate phenomenon known as the El Niño–Southern Oscillation (ENSO) cycle, which also includes its cool counterpart, La Niña (Trenberth, 1997). During this El Niño event, the southwestern and southern United States, including Tucson, experienced higher than average precipitation December through February (L'Heureux et al., 2024). El Niño events may also have influenced the 1930-1933 winter data of Humphrey. A moderate El Niño event occurred in 1930 and a weak event occurred in 1932 (Andrade & Sellers, 1988).

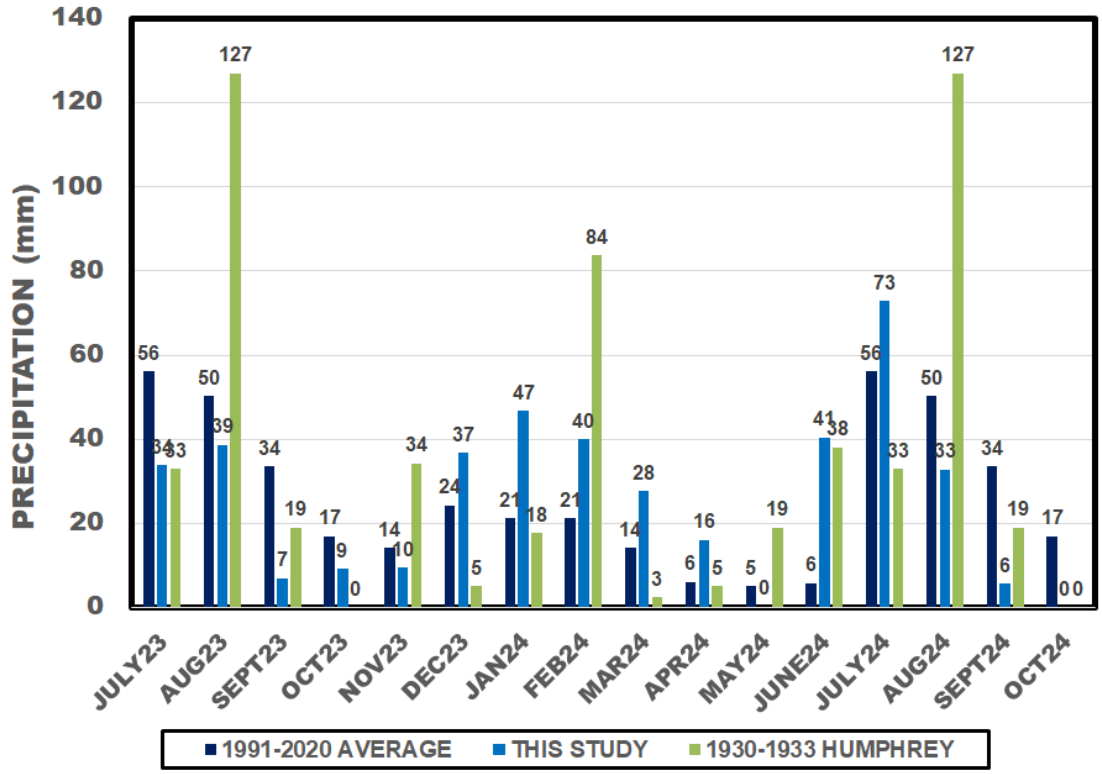

Fig. 4. Rain Gauge data comparison
Sources: own elaboration based on Humphrey (1933) and National Weather Service (2025)

Storm events. We catalogued 24 storm events during the 18 month study: 10 monsoon storms and 14 winter storms. The linear robust multivariate regression models are statistically significant in 18 of the 24 storm events (Table 4). The regression models were significant for nine winter storms, showing that precipitation from less localized winter storms can also vary spatially. Twelve of the 18 statistically significant regression models had at least one variable or the intercept that were also statistically significant. Latitude was statistically significant in eight regression models.

Figure 5 contains interpolated maps of the three most intense monsoon storms, and Figure 6 shows the three most intense winter storms. All three monsoon storms had the most intense precipitation in the south to southwest portion of the study area, which may be due to the prevailing south to southwesterly winds during the monsoon (Yang et al., 2016). The July 24–29, 2024 storm event also has intense precipitation in the northeast corner of the study area, which we attribute or orographic precipitation (Baghanam et al. 2025). The community science study of Crimmins et al. (2021) observed both these effects in some of the storm events they documented.

Table 4. Storm event analysis of precipitation (mm)

Dates	N	Average	Maximum	Zeros	Significant	Significant Variables
17-18 July23	121	10	38	11	yes	Lat, Z, Int
21 July-1 Aug23	121	28	162	1	yes	None
17-23 Aug23	125	26	75	None	yes	Lat
25-27 Aug23	125	4	28	51	yes	None
30 Aug-2 Sept23	111	3	21	32	yes	Canopy
12-14 Sept23	113	4	23	25	yes	Lat, Z, Int
24-26 Oct23	112	6	51	22	yes	Canopy
16-19 Nov23	113	6	35	12	yes	None
24-26 Nov23	113	4	24	22	yes	Lat
1-2 Dec23	110	5	64	17	yes	None
22-24 Dec23	111	31	51	3	yes	None
2-5 Jan24	106	2	25	43	yes	None
7-8 Jan24	105	2	25	34	no	None
21-25 Jan24	104	41	76	5	no	None
1-3 Feb24	100	12	50	8	no	None
6-11 Feb24	99	18	43	2	no	None
26-29 Feb24	98	7	19	14	yes	Z
7-9 March24	92	12	44	12	yes	Lat
23-27 March24	92	10	28	12	no	None
31 Mar.-2 Apr24	91	21	43	7	yes	Lat, Lon, Int
21-25 June24	86	33	89	6	yes	Lat
24-29 July24	85	36	72	8	yes	Int
17-24 Aug24	84	16	50	6	yes	Lat, Lon, Z, Int
15-17 Sept24	86	3	13	19	no	None

Source: own elaboration

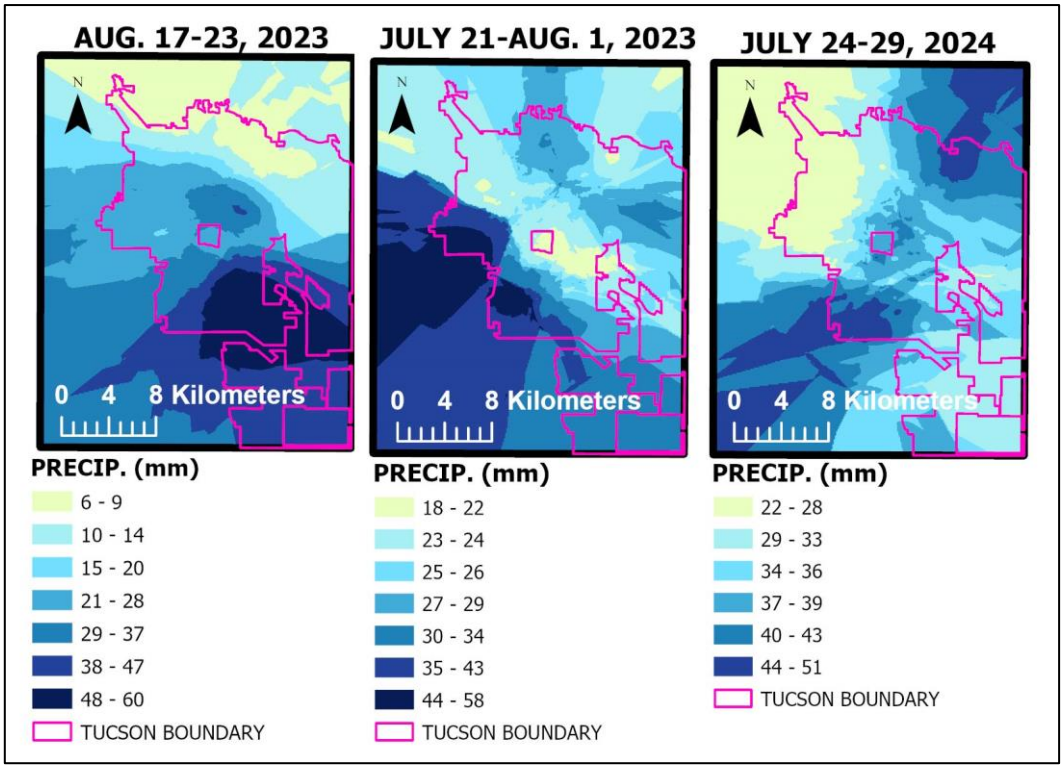

Fig. 5. Three most intense summer monsoon storms
Source: own elaboration using community data

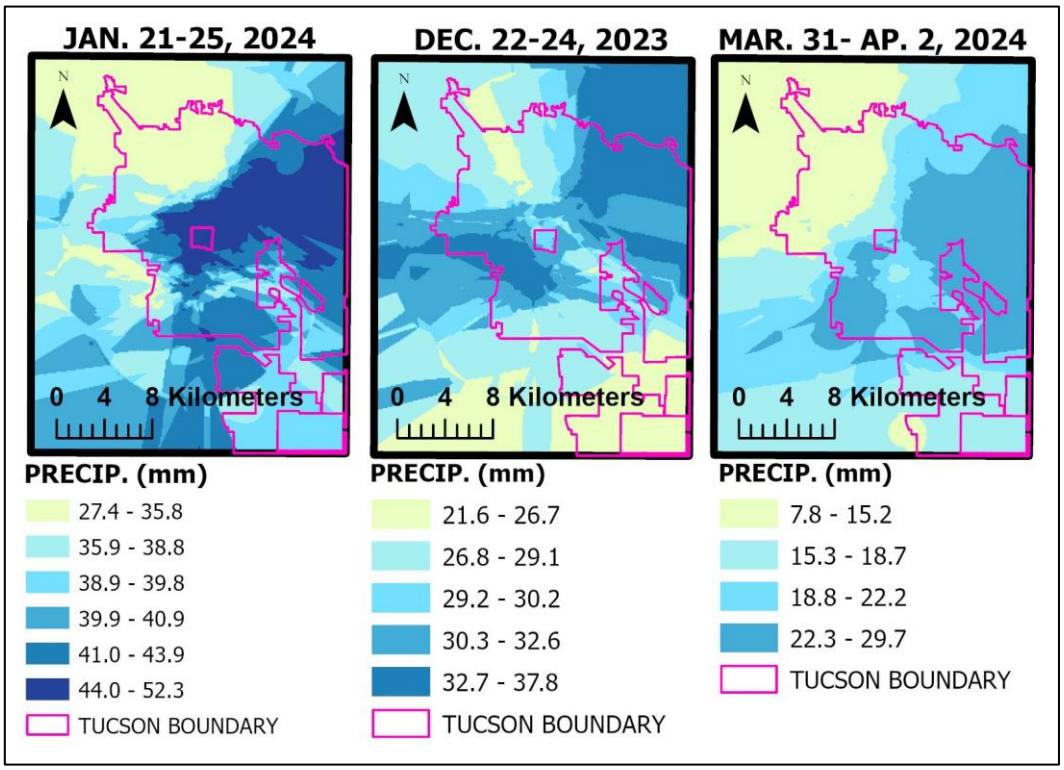

Fig. 6. Three most intense winter storms
Source: own elaboration using community data

Seasonal analysis. Figure 7 shows precipitation maps of the 2023 monsoon, 2024 monsoon, and 2023–24 winter. The GLM was statistically significant for the 2023 monsoon, with longitude, elevation, and the intercept as significant explanatory variables. The GLM's for winter, 2024 monsoon, and the study total were not statistically significant. The average 2024 monsoon precipitation is almost twice as high as the 2023 monsoon precipitation (Table 5). Because the data were not normally distributed, we used the non-parametric Wilcoxon rank-sum test to test for the difference between the 67 data pairs in common, and the difference between Monsoon 2023 and Monsoon 2024 is highly significant ($p<0.001$).

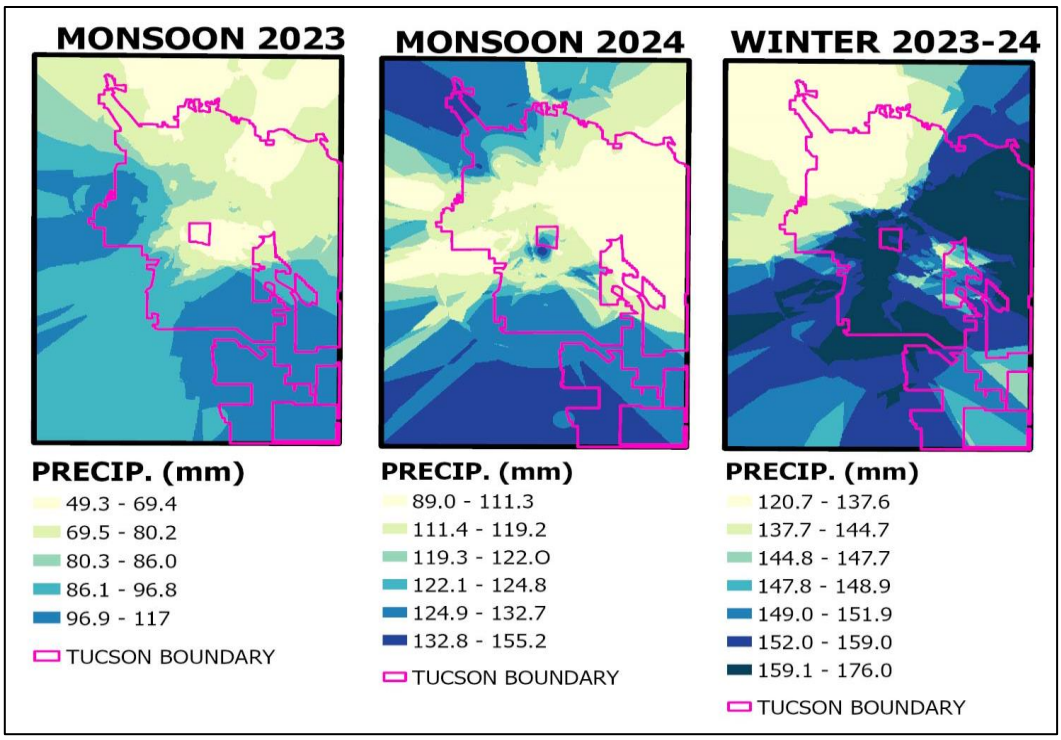

Fig. 7. Seasonal precipitation
Source: own elaboration using community data

Table 5. Seasonal rain gauge data

Season	GLM Sig.	n	Avg.	Stdev.	Min.	Max.	Range	SE
Monsoon 2023	yes	105	80	25	12	173	161	2.4
Winter 2023-24	no	87	152	35	12	310	298	3.7
Monsoon 2024	no	67	115	38	24	268	243	4.7
Study Total	no	67	419	69	191	635	444	8.4

Source: own elaboration

Total precipitation. Figure 8 shows the total precipitation of the 67 participants who submitted rain gauge data every month. We found that the south and southwest quadrants of the study area received the most precipitation. There is also an area of moderate precipitation in the northeast quadrant of the study area. We used the non-

parametric Wilcoxon rank-sum test to evaluate whether these differences were statistically significant. We found no significant difference between the north and south rain gauges (p=0.38). We also found no statistical difference between the east and west rain gauges (p=0.80).

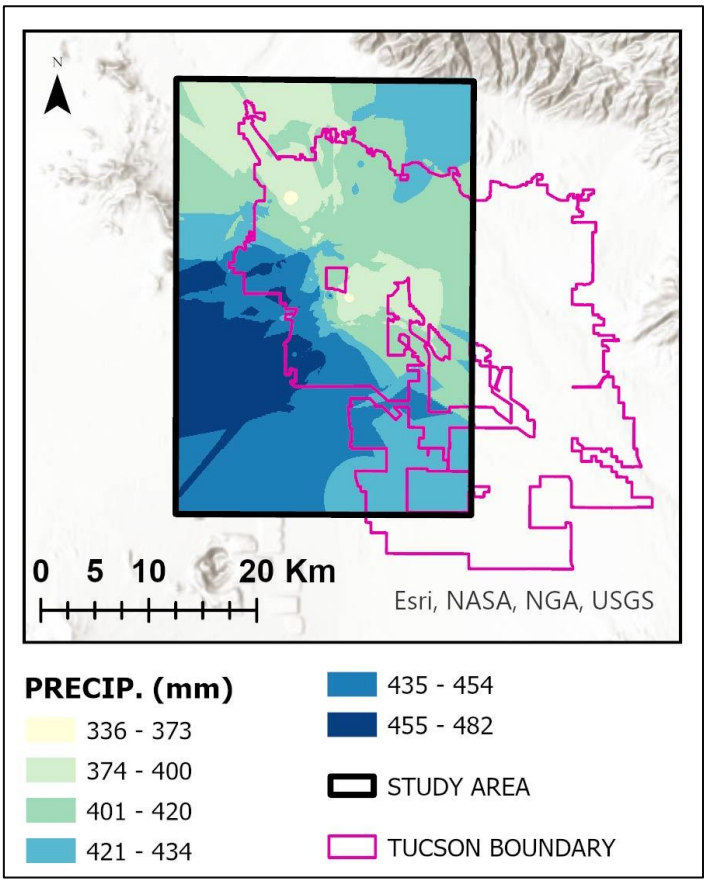

Fig. 8. Total precipitation
Source: own elaboration using community data

GPM IMERG-rain gauge comparison: chi-square, bias, and RMSE. Only three chi-squared values are less than the 1.0 mm limit that indicates statistical agreement between the GPM and rain gauge measurements (Fig. 9). Twelve chi-squared values are in the marginal agreement range of 1.1-4.0 mm. The chi-squared values exceeded the 4.0 mm limit in September 2023, October 2023, and October 2024. GPM IMERG overestimated the amount of precipitation in September and October 2023. The highest chi-squared value of 86.4 was measured in October 2024, a month with almost no precipitation in the study area.

The overall bias is 6 mm, indicating that on average GPM IMERG overestimates the precipitation in Tucson (Fig. 10). The bias is 7 mm during the North American monsoon, and 11 mm during the winter rainy season. The drier fall and spring months show a smaller bias of 3 mm. There are negative biases at the start of the monsoon and frontal rainy seasons.

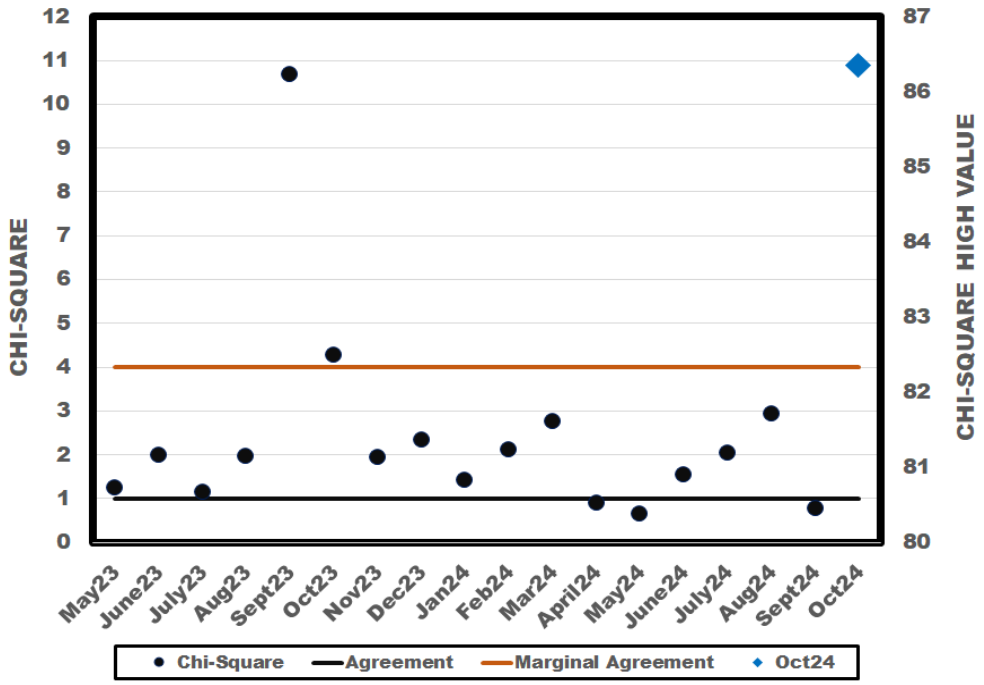

Fig. 9. Monthly chi-square
Source: own elaboration

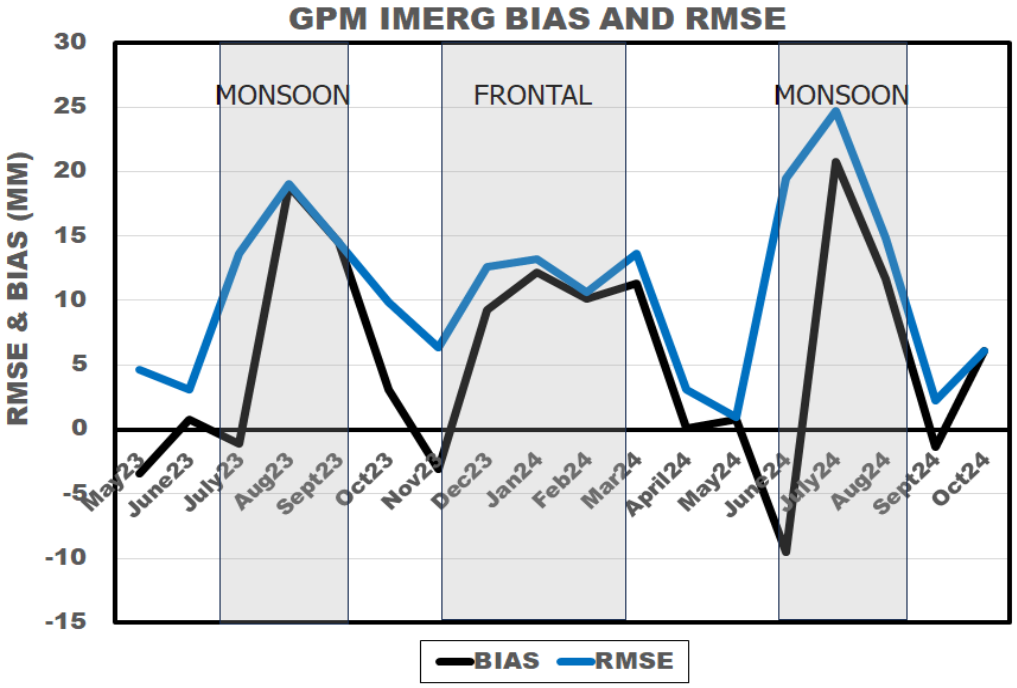

Fig. 10. Bias and RMSE
Source: own elaboration

We measured an overall RMSE of 13 mm. The RMSE is 17 mm during the monsoon months of June, July, and August; 13 mm during the frontal rainy season of December-March; and 7 mm during the drier fall and spring months. We attribute the higher monsoon RMSE to the higher spatial variability of convective monsoon storms compared to the frontal storms of the winter rainy season (Comrie & Broyles 2002).

Conclusions

We conducted an in-depth analysis of Tucson area precipitation with community scientist rain gauge measurements. The southern part of the study area had more precipitation, but the difference was not statistically significant. We also compared our data to four Tucson weather stations, the Pima Regional Flood District and 1991-2020 historic norms. We found no statistically significant differences between the four datasets.

Our regression analysis of Tucson storm events illustrates how Sonoran Desert precipitation is highly variable in intensity as well as through space and time. We used latitude, longitude, elevation, and percent tree canopy as explanatory variables. Similar to Comrie and Boyles (2002), we found that latitude, longitude or elevation were significant explanatory variables for half of the storm events. Percent tree canopy was a significant explanatory variable for two storm events.

Ground-based data like this study are essential for validating satellite precipitation in semi-arid areas (Ehsani et al. 2022). The GPM IMERG has an overall bias of +6 mm in comparison to rain gauge data. We attribute this partially to virga, the evaporation of rain before it reaches the ground. GPM IMERG uses infrared and passive microwave data to measure precipitation in the atmosphere. The IMERG algorithm may misidentify virga as surface precipitation, especially in arid zones like the southwestern U.S (Sutton et al. 2024). Wang et al. (2018) found that virga may account for more than 30% of the precipitation in the western United States.

This study illustrates how community science can address community concerns such as precipitation, while also providing valuable data to scientists studying the issue. We recruited low income and Spanish speaking participants, who are not easily reached with conventional science outreach. One hundred twelve or 67% of the participants met U.S. Department of Housing and Urban Development (HUD) criteria for being low income. Forty-three percent of the participants spoke Spanish as their primary language, and 60% of participants identified as Hispanic.

Funding and acknowledgements

This research was funded by the National Aeronautics and Space Administration (NASA), grant number 21-EEJ21-0014. We wish to thank the community scientists and Pima County Regional Flood Control District for providing data.

Declaration of competing interests

The authors declare that they have no known competing financial interests or personal relationships that could have appeared to influence the work reported in this paper.

Data availability

The datasets used and analyzed during the current study are available from the corresponding author upon request.

Use of generative AI and AI-assisted technologies

Generative AI was not used for the data analysis, creating maps and figures, or writing the manuscript.

References

Adams D.K., Comrie A.C. (1997). The north American monsoon. Bulletin of the American Meteorological Society, 78(10), 2197–2214.

Ahrens B. (2006). Distance in spatial interpolation of daily rain gauge data. Hydrology and Earth System Sciences, 10(2), 197–208.

Andrade Jr E.R., Sellers W.D. (1988). El Niño and its effect on precipitation in Arizona and western New Mexico. Journal of Climatology, 8(4), 403–410.

Arizona State University Map and Geospatial Hub (Cartographer) (n.d.). Arizona state-wide digital elevation model (NAD 1927).

Ault T.R., Mankin J.S., Cook B.I., Smerdon J.E. (2016). Relative impacts of mitigation, temperature, and precipitation on 21st-century megadrought risk in the American Southwest. Science Advances, 2(10), e1600873.

Baghanam A.H., Mohebbi A. (2025). Understanding orographic precipitation pattern in Arizona: Implications for climate change. Journal of Hydrology: Regional Studies, 62. https://doi.org/10.1016/j.ejrh.2025.102793.

Bostan P. (2017). Basic kriging methods in geostatistics. Yuzuncu Yıl University Journal of Agricultural Sciences, 27(1), 10–20.

Castro C.L., Beltrán-Przekurat A.B., Pielke Sr R.A. (2009). Spatiotemporal variability of precipitation, modeled soil moisture, and vegetation greenness in North America within the recent observational record. Journal of Hydrometeorology, 10(6), 1355–1378.

Cheng K.S., Lin Y.C., Liou J.J. (2008). Rain-gauge network evaluation and augmentation using geostatistics. Hydrological Processes: An International Journal, 22(14), 2554–2564.

City of Tucson (2024). 2023 Annual Water Quality Report. Retrieved from Tucson, Arizona.

Comrie A.C. (2000). Mapping a wind-modified urban heat island in Tucson, Arizona (with comments on integrating research and undergraduate learning). Bulletin of the American Meteorological Society, 81(10), 2417–2432.

Comrie A.C., Broyles B. (2002). Variability and spatial modeling of fine-scale precipitation data for the Sonoran Desert of south-west Arizona. Journal of Arid Environments, 50(4), 573–592.

Conrad C.C., Hilchey K.G. (2011). A review of citizen science and community-based environmental monitoring: issues and opportunities. Environmental monitoring and assessment, 176, 273–291.

Crimmins M.A., McMahan B., Holmgren W.F., Woodard G. (2021). Tracking precipitation patterns across a western US metropolitan area using volunteer observers: RainLog. Org. International Journal of Climatology, 41(8), 4201–4214.

Drożdzioł R., Absalon D. (2023). Evaluation of Selected Amateur Rain Gauges with Hellmann Rain Gauge Measurements. Climate, 11(5), 107.

Earls J., Dixon B. (2007). Spatial interpolation of rainfall data using ArcGIS: A comparative study. Proceedings of the 27th Annual ESRI International User Conference.

Ehsani M.R., Heflin S., Risanto C.B., Behrangi A. (2022). How well do satellite and reanalysis precipitation products capture North American monsoon season in Arizona and New Mexico? Weather and Climate Extremes, 38, 100521.

Esri (Cartographer) (2024). Global Landsat GLS 15m panchromatic and multitemporal imagery with on-the-fly renderings and indices for visualization and analysis. https://www.arcgis.com/home/item.html?id=67d71f5e453f40cbb27e423ca7071cc1.

Esri (2025). What is empirical Bayesian kriging? https://pro.arcgis.com/en/pro-app/latest/help/analysis/geostatistical-analyst/what-is-empirical-bayesian-kriging-.htm.

Foley T., Wolf A.M., Henriquez P., Sandoval F., Rogstad A. (2019). Low income urban forestry program in Tucson, Arizona, USA. Cities and the Environment (CATE), 12(2), 2.

Ghasemi Tousi E., O'Brien W., Doulabian S., Shadmehri Toosi A. (2021). Climate changes impact on stormwater infrastructure design in Tucson Arizona. Sustainable Cities and Society. https://doi.org/10.1016/j.scs.2021.103014.

Gonzalez P., Garfin G.M., Breshears D.D., Brooks K.M., Brown H.E., Elias E.H., Gunasekara A., Huntly N., Maldonado J.K., Mantua N.J., Margolis H.G., McAfee S., Middleton B.R., Udall B.H. (2018). Chapter 25: Southwest. Retrieved from Washington, DC, USA.

Gupta A., Kamble T., Machiwal D. (2017). Comparison of ordinary and Bayesian kriging techniques in depicting rainfall variability in arid and semi-arid regions of north-west India. Environmental Earth Sciences, 76(15), 512.

Haggag M., Elsayed A.A., Awadallah A.G. (2016). Evaluation of rain gauge network in arid regions using geostatistical approach: case study in northern Oman. Arabian Journal of Geosciences, 9(9), 552. https://doi.org/10.1007/s12517-016-2576-6.

Humphrey R.R. (1933). A detailed study of desert rainfall. Ecology, 14(1), 31–34.

Kelley O. (2020). The IMERG multi-satellite precipitation estimates reformatted as 2-byte GeoTIFF files for display in a Geographic Information System (GIS).

Kumar M. (1988). World geodetic system 1984: A modern and accurate global reference frame. Marine Geodesy, 12(2), 117–126.

L'Heureux M.L., Harnos D.S., Becker E., Brettschneider B., Chen M., Johnson N.C., Kumar A., Tippett M.K. (2024). How well do seasonal climate anomalies match expected El Niño–Southern Oscillation (ENSO) impacts? Bulletin of the American Meteorological Society, 105(8), E1542-E1551.

Li J., Heap A.D. (2011). A review of comparative studies of spatial interpolation methods in environmental sciences: Performance and impact factors. Ecological Informatics, 6(3–4), 228–241.

Liu L., Schaefer K., Zhang T., Wahr J. (2012). Estimating 1992–2000 average active layer thickness on the Alaskan North Slope from remotely sensed surface subsidence. Journal of Geophysical Research: Earth Surface, 117(F1).

Mazon J.J., Castro C.L., Adams D.K., Chang H.-I., Carrillo C.M., Brost J.J. (2016). Objective climatological analysis of extreme weather events in Arizona during the North American monsoon. Journal of Applied Meteorology and Climatology, 55(11), 2431–2450.

Meng Q., Liu Z., Borders B.E. (2013). Assessment of regression kriging for spatial interpolation–comparisons of seven GIS interpolation methods. Cartography and geographic information science, 40(1), 28–39.

Milton J.S. (1999). Statistical Methods in the Biological and Health Sciences. Boston, MA: McGraw-Hill.

NASA (2025). NASA's Global Precipitation Measurement (GPM) Mission. https://arthurhouhttps.pps.eosdis.nasa.gov/gpmdata/.

National_Weather_Service (2025). Tucson Monthly and Daily Normals and Records. https://www.weather.gov/twc/TucsonMonthlyNormalExtremes.

Northeast Regional Climate Center (NRCC) (2026). http://climod2.nrcc.cornell.edu/.

Overpeck J.T., Udall B. (2020). Climate change and the aridification of North America. Proceedings of the national academy of sciences, 117(22), 11856–11858.

Peng Q., Xie S.-P., Miyamoto A., Deser C., Zhang P., Luongo M.T. (2025). Strong 2023–2024 El Niño generated by ocean dynamics. Nature Geoscience, 1–8.

Pima Association of Governments (PAG). (2008). Regional Tree Canopy. https://maps.pagregion.com/PAG-GIMap/Documents/GIToolDataSources.pdf.

Pima_County_Regional_Flood_Control_District. (2026). ALERT System Flood Warning Map. https://alertmap.rfcd.pima.gov/gmap/gmap.html.

Raczka, B.M., Davis K.J., Huntzinger D., Neilson R.P., Poulter B., Richardson A.D., Xiao J., Baker I., Ciais P., Keenan T.F. (2013). Evaluation of continental carbon cycle siulations with North American flux tower observations. Ecological Monographs, 83(4), 531–556.

Schaefer K., Liu L., Parsekian A., Jafarov E., Chen A., Zhang T., Gusmeroli A., Panda S., Zebker H.A., Schaefer T. (2015). Remotely Sensed Active Layer Thickness (ReSALT) at Barrow, Alaska Using Interferometric Synthetic Aperture Radar. Remote Sensing, 7(4), 3735–3759.

Seager R., Ting M., Held I., Kushnir Y., Lu J., Vecchi G., Huang, H.-P., Harnik N., Leetmaa A., Lau N.-C. (2007). Model projections of an imminent transition to a more arid climate in southwestern North America. Science, 316(5828), 1181–1184.

Silvertooth J.C.C.R.S.J.N., article, V.N., vol. 16, no. 12. Tucson: 2025. http://hdl.handle.net/10150/678219 (2025). Colorado River Status – June 2025. University of Arizona VegIPM Newsletter, 16(12).

Sutton J.R.P., Kirschbaum D., Stanley T., Orland E. (2024). Evaluating Precipitation Events Using GPM IMERG 30-Minute Near-Real-Time Precipitation Estimates. Journal of Hydrometeorology, 25(7), 991-1006. https://doi.org/10.1175/JHM-D-23-0141.1.

Trenberth K.E. (1997). The definition of el nino. Bulletin of the American Meteorological Society, 78(12), 2771–2778.

Udall B., Overpeck J. (2017). The twenty-first century Colorado River hot drought and implications for the future. Water Resources Research, 53(3), 2404–2418.

Villagómez-Márquez N., Abrell L., Foley T., Ramírez-Andreotta M.D. (2023). Organic micropollutants measured in roof-harvested rainwater from rural and urban environmental justice communities in Arizona. Science of the Total Environment, 876, 162662.

Wang Y., You Y., Kulie M. (2018). Global virga precipitation distribution derived from three spaceborne radars and its contribution to the false radiometer precipitation detection. Geophysical Research Letters, 45(9), 4446–4455.

Wei S., Wang Y., Xu T., Buzzard V.R., McCormick G., Yang B., Xia T., Wang Z.-H. (2026). Machine learning-based multi-objective optimization of smart irrigation of urban trees in Arizona. Landscape and Urban Planning, 267. https://doi.org/10.1016/j.landurbplan.2025.105539.

Weiss J.L., Castro C.L., Overpeck J.T. (2009). Distinguishing pronounced droughts in the southwestern United States: Seasonality and effects of warmer temperatures. Journal of Climate, 22(22), 5918–5932.

Weiss J.L., Overpeck J.T. (2005). Is the Sonoran Desert losing its cool? Global Change Biology, 11(12), 2065–2077.

Yang Z., Dominguez F., Gupta H., Zeng X., Norman L. (2016). Urban effects on regional climate: A case study in the Phoenix and Tucson "Sun Corridor". Earth Interactions, 20(20), 1–25.

Yu C., Yao W. (2017). Robust linear regression: A review and comparison. Communications in Statistics-Simulation and Computation, 46(8), 6261–6282.